Scalar resonances in the $D^+ \to K^- K^+ K^+$ decay

L. Roca[*]

Departamento de Física, Universidad de Murcia, E-30071 Murcia, Spain

E. Oset[†]

Departamento de Física Teórica and IFIC, Centro Mixto Universidad de Valencia-CSIC
Institutos de Investigación de Pate rna, Aptdo.22085, 46071 Valencia, Spain

We study theoretically the resonant structure of the double Cabibbo suppressed $D^+ \to K^- K^+ K^+$ decay. We start from an elementary production diagram, considered subleading in previous approaches, which cannot produce a final $K^- K^+$ pair at the tree level but which we show to be able to provide the strength of the decay through final meson-meson state interaction. The different meson-meson elementary productions are related through SU(3), and the final rescattering is implemented from a suitable implementation of unitary extensions of chiral perturbation theory, which generate dynamically the scalar resonances $f_0(980)$ and $a_0(980)$. We obtain a good agreement with recent experimental data from the LHCb Collaboration with a minimal freedom in the fit and show the dominance of the $a_0(980)$ contribution close to the threshold of the $K^- K^+$ spectrum.

I. INTRODUCTION

Weak decay of heavy mesons into hadrons has become an important source of information on the hadron-hadron interaction. In particular, the decay of D mesons into three pseudoscalars has drawn the attention of different groups with the aim of learning about the meson-meson interaction [1–6]. These works deal with the $D \to K\pi\pi$ decay, which is Cabibbo favored and is mainly used to learn about the $\pi\pi$ interaction. Other D decays are studied in Ref. [7], using the $D \to \pi^+\pi^+\pi^-$ and $D \to \pi^+K^+K^-$ reactions to learn about the $\pi\pi$ and $K\bar{K}$ interaction; in Refs. [8,9], interpreting the $D_s^+ \to \pi^+\pi^0\eta$ decay; in Ref. [10], studying the single Cabibbo suppressed $D^+ \to \pi^+\pi^0\eta$ decay; or in Ref. [11], studying the $D_s^+ \to \pi^+\pi^0 a_0(980)(f_0(980))$ reactions. The $D^0 \to K^-\pi^+\eta$ reaction is also studied in Ref. [12] from which information on the $a_0(980)$ and $\kappa(K_0^*(700))$ is obtained.

The reaction that we study here is $D^+ \to K^- K^+ K^+$, which is doubly Cabibbo suppressed but can teach us much about the $K\bar{K}$ interaction, one of the pseudoscalar interaction channels most poorly known. The reaction is studied

---

[*]luisroca@um.es
[†]oset@ific.uv.es

by the LHCb Collaboration in Ref. [13] and analyzed using two methods, the standard one, the isobar model, and then the triple-M model developed in Ref. [14]. The isobar model is the standard method used in the LHCb analysis and in most of the experimental collaborations. The full decay amplitude is written in terms of the only two independent variables

$$T(s_{12}, s_{13}) = c_{NR} + \sum_k c_k T_k(s_{12}, s_{13}), \qquad (1)$$

where c_{NR} is a nonresonant background term and T_k are intermediate resonant amplitudes properly parametrized. The parameters in the different terms and the complex weights c_k are obtained by performing a best fit to the Dalitz plot data. The method is efficient to extract information on the role played by different resonances but has its limitations. We quote Ref. [14]: "This approach, albeit largely employed [15], has conceptual limitations. The outcome of isobar model analyses are resonance parameters such as fit fractions, masses and widths, which are neither directly related to any underlying dynamical theory nor provide clues to the identification of two-body substructures. Thus, the systematic interpretation of the isobar model results is rather difficult."

Steps to make different analyses of the data to allow a better matching with theoretical tools used in the study of meson interactions are done in Ref. [16], and tools to use three-body dynamics have also been used in the $D \to K\pi\pi$ reactions [1,2,17–19]. Yet, the majority of analyses rely
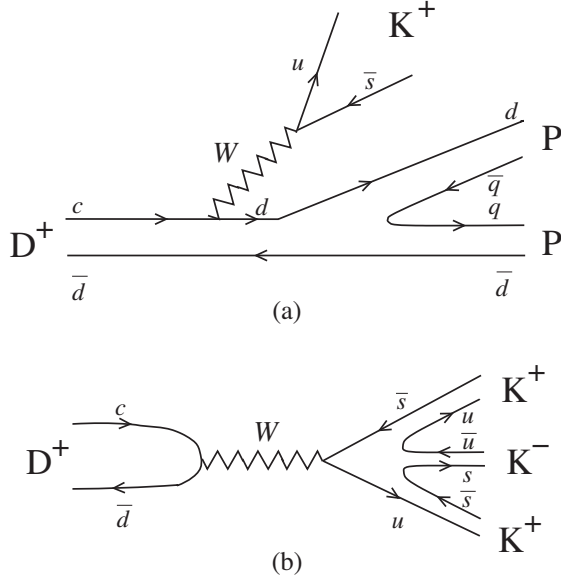
FIG. 1.   Elementary $D^+ \to K^+ PP$ process at the quark level.

upon the consideration of two-body amplitudes having one of the mesons as spectator, and this is also used in Ref. [14]. The fact that the three-body amplitudes can be constructed from on-shell two-body amplitudes, since of-shell parts are shown to cancel with contact terms present in the theory, makes this approach more realistic [20,21]. However, there are other reasons to neglect terms involving explicitly three particles interacting because after the interaction of a pair of mesons in regions where a resonance appears to be important, the resulting invariant mass of one of the particles of the pair with the third one does not have a given value but usually spans a large region of invariant mass, thus diluting the possible contribution of another resonance, which, however, is taken into consideration with the direct interaction of this original pair considering the third particle as a spectator.

The work of Ref. [14] uses effective Lagrangians to deal with the weak and strong interaction. For the weak interaction, the starting point is the diagram of Fig. 1(b), which involves quark pair annihilation (W annihilation). The diagram of Fig. 1(a), which involves external emission, is considered as a possible mechanism, but it does not provide $K^- K^+ K^+$ upon hadronization of the quarks, and final state interaction is needed to produce this state. For this reason, it is neglected in the analysis of Ref. [14], and the annihilation mechanism of Fig. 1(a) is used as the starting point. The mesons stemming from the double hadronization of this mechanism are allowed to follow final state interaction. The final state interaction of the mesons in Ref. [14] is done using Lagrangians of Ref. [22], in which chiral perturbation is used, including resonances explicitly. Yet, extra unitarization is considered in Ref. [14], using techniques of the chiral unitary approach of Refs. [23–25], which justifies that the parameters that

they get from a fit to the data are not the parameters used in Ref. [22]. The unitarization is, however, done with one approximation with respect to the former works, using the K-matrix approach in which the real part of the loop functions is neglected and only the imaginary part is kept. The use of the K-matrix approach has one intrinsic problem, which is that ignoring the real part of the loops prevents resonances being dynamically generated. This is why they have to be introduced by hand, and the approach cannot tell us about the nature of these resonances. However, resonances like the $f_0(980)$ and $a_0(980)$ appear as a consequence of the meson-meson interaction in the chiral unitary approach of Refs. [23–25], and the consistency of the approach with data gives support to this picture. We should mention that in a recent work [26] the authors of Ref. [14] already considered the real parts of the loops.

In the present approach to the $D^+ \to K^- K^+ K^+$ reaction, we only have three parameters to fit to the data: the global strength, the strength of the ϕK^+ production amplitude, and a relative phase of the s-wave to p-wave mechanisms. Since the global strength is irrelevant when we compare to events in the data, and the global strength of the ϕK^+ is easily determined from the clean peak in the $K^+ K^-$ mass distribution, our approach has basically 1 degree of freedom to fit all the data. This contrasts with the ten free parameters that one has in the approach of Ref. [14]. The isobar model has even more parameters.

We have here two of the most important differences between the work of Ref. [14] and that we present here. The starting point for us is not the diagram of Fig. 1(b) but the one of Fig. 1(a). The reason is the following: in the classification of weak decay topologies of Refs. [27,28], the order of importance is external emission, internal emission, W exchange, and annihilation. Given the fact that the $K\bar{K}$ interaction at low energies is driven by the $f_0(980)$ and $a_0(980)$ resonances, the final state interaction is very important and does not destroy the order of the primary decays. In the analysis of the BESIII data for $D_s^+ \to \pi^+ \pi^0 \eta$, [29], the process removing the $\rho^+ \eta$ channel was supposed to proceed via W annihilation with a rate of an order of magnitude bigger than for usual W-annihilation processes. Yet, the decay is studied in Ref. [8] with an approach similar to the one we follow here, and it was shown that the process proceeded via internal emission and final state interaction.

Our approach to these weak processes consist in a first identification of the dominant mechanisms at the quark level; then, we proceed with hadronization to produce the mesons that appear in a first step and then consider the final state interaction of these mesons to produce at the end the desired final state. We must take into account that the hadronization, including new $q\bar{q}$ pairs to produce mesons, results in a reduction factor in the decay amplitude. Then, in the mechanism of Fig. 1(b) used in Ref. [14], one has two

hadronizations, while in the mechanism that we have of Fig. 1(a), there is only one hadronization. All these reasons justify that we neglect the mechanism of Fig. 1(b) and start the process with the one of Fig. 1(a). The choice of the starting mechanism is not innocuous; different initial meson channels are produced, which upon final state interaction give rise to the three kaons. This means that coupled channels have to be used in the approach, as also done in Ref. [14], but the amount $f_0(980)$ or $a_0(980)$ production, for instance, depends on the mechanisms assumed and the weights by which the different meson channels appear in the hadronization.

As we mentioned, in the experiment of Ref. [13], two methods of analysis were made, the first one using the isobar model and the other one using the formalism of Ref. [14]. The problems using the isobar model which are exposed in Ref. [14] are further evidenced in the study done in Ref. [13]. Indeed, when using the isobar model, three options, A, B, and C, are used. In model A, they include the ϕK^+, $f_0(980)K^+$, and $f_0(1370)K^+$ channels. In model B, they add a nonresonant amplitude. In model C, they replace the $f_0(1370)K^+$ channel by the $a_0(980)K^+$ one. They note that both models B and C are equally acceptable. This means that this type of analysis cannot tell us about the relevance of the $a_0(980)$ resonance in this reaction. On the contrary, the analysis done there using the model of Ref. [14] shows a dominant role played by the $a_0(980)$ resonance. Incidentally, we should also mention that by using fully unitarized amplitudes in coupled channels in the approach that we follow we do not have to worry about background. The amplitudes contain the resonance pole but provide at the same time background terms away from the resonance peaks.

The strategy of our work, which is widely used (see Ref. [30] for a review on this issue), is to establish the dominant mechanisms at the quark level that produce the desired number of mesons after hadronization including $q\bar{q}$ pairs with the quantum numbers of the vacuum. Then, all pairs of mesons are allowed to undergo final state interaction, keeping a third particle as a spectator. The amplitudes are properly symmetrized to account for the identity of the particles. The final sate interaction requires to use the meson-meson scattering amplitudes, which we take from the prior study with the chiral unitary approach. This method has a minimum input, basically a global strength and some relative strength from the s-wave to p-wave amplitudes. An agreement with data with this minimum input is considered as giving support for the chiral unitary approach to the meson-meson interaction and in particular for the nature of some of the resonances that it provides as dynamically generated from the meson interaction rather than genuine states of particular quark configurations. The good agreement with data that we will show in the present work will then give support to this kind of molecular picture for the $f_0(980)$ and $a_0(980)$ resonances, which

adds to the support from many other reactions where these states are produced [30].

This is not the place for a review of the abundant work on the scalar resonances, but a few comments on our present perspective can be opportune. Early work on the nature of the $\sigma(f_0(500))$, $f_0(980)$, and $a_0(980)$ resonances is done in Refs. [31–40]. Data on meson scattering, $\gamma\gamma \to \pi\pi$, $\phi \to \pi^0\pi^0\gamma$, $\pi^0\eta\gamma$, etc., are studied, and while the input and technical details are different, there is a basic coincidence that these resonances are not ordinary $q\bar{q}$ states. The σ meson was originally introduced by Schwinger [41] long before the advent of QCD and played a crucial role for the construction of a chirally symmetric pion-nucleon Lagrangian in the linear sigma model of Gell-Mann and Levy [42]. Later, the light scalars were accommodated within a $qq\bar{q}\bar{q}$ picture within the MIT quark bag model [43]. Some phenomenological consequences of the four-quark picture can be found in Refs. [44,45]. Early works such as Refs. [31–33] would emphasize that, even starting from a $q\bar{q}$ seed, when this couples to meson-meson components, the meson cloud takes a predominant role in low energy reactions, emphasizing the non-$q\bar{q}$ nature of these states. Recent works on different reactions conclude the four-quark nature of these resonances [46–48] by showing inconsistencies on the use of direct coupling of the resonances to $q\bar{q}$ components. A unifying picture that shares the basic conclusions of former and recent works is the chiral unitary approach [49–52]. The work starts by acknowledging that the chiral Lagrangians [53,54] implement an effective representation of QCD at low energy in terms of the Goldstone mesons as elementary fields. The contents of the chiral Lagrangians are extended to intermediate energies by using them as kernels in different unitary approaches in coupled channels using the Bethe-Salpeter equation in Refs. [49–52], dispersion relations in Ref. [23], or the inverse amplitude method in Ref. [24] (see a recent comparison of these methods in Ref. [55]). Independent of the method, the unitarization in coupled channels gives rise to meson-meson scattering amplitudes, with good analytical properties, exact unitarity, and singularities that show up as poles in the Riemann complex plane. The $\sigma(f_0(500))$, $f_0(980)$, and $a_0(980)$ appear as poles of these scattering matrices in this approach. The predictions, compared with the data, are very good, not only in meson-meson phase shifts but also in a large amount of different reactions, including $\phi \to \pi\pi\gamma$, $\pi\eta\gamma$, $\gamma\gamma \to \pi\pi$, weak decays of D and B mesons, etc. (see reviews in Refs. [30,56–58]). Given the fact that the low-lying scalar resonances are obtained from the meson-meson interaction and not from the quark-quark interaction, these resonances are usually referred to as dynamically generated resonances, to emphasize the fact that the meson-meson interaction is what produces them in this approach. The approach thus shares with Refs. [46–48] the conclusion that there is not direct coupling to $q\bar{q}$

components. This fact is interpreted in these latter works as a proof that the $f_0(500)$, $f_0(980)$, and $a_0(980)$ are four-quark states. Certainly, the picture stemming from the meson-meson interaction can also be interpreted in this way since two mesons would have four quarks, but the knowledge of the actual and detailed quark composition is unnecessary in that picture because all reactions where these resonances are produced proceed via the primary production of the basic meson-meson components followed by their posterior interaction where the resonances are generated. The meson-meson wave functions in coordinate space are also unnecessary to study any reaction, but the formalism to evaluate them has been developed and applied for some cases [59,60].

II. FORMALISM

As briefly discussed in the Introduction, the possible elementary quark topologies at tree level for the $D^+ \rightarrow K^- PP$ process, where PP stands for a pseudoscalar meson pair, are depicted in Fig. 1. Note that PP in Fig. 1(a) cannot be K^+K^- at the tree level since it cannot be produced from $\bar{d}d$, but the K^+K^- pair can be produced via final state interaction (FSI) of the pseudoscalar pair. This necessity for FSI was the main reason for neglecting the diagram (a) in Ref. [14], which is the basis of the LHCb experimental analysis in Ref. [13]. However, our position in the present work is opposite, and we are going to argue why we expect the (a) diagram to be dominant. First, diagram (b) represents annihilation, and since the D have spin zero, the W-annihilation diagram is suppressed by helicity conservation at the light quark vertex [28]. In addition, diagram (b) requires two hadronizations, each of which reduces the width by about 1 order of magnitude [61]. Furthermore, diagram (a) relies upon external emission, which has the largest strength for weak interaction [28]. Indeed, one quark is operative, and the other one remains a spectator, which implies a one-body operator, versus the two-body operator required in the annihilation, and is color favored. On the other hand, the FSI interaction necessary to produce final K^+K^- is actually required at low invariant masses since that region is very influenced by the $a_0(980)$ and $f_0(980)$ resonances, which are dynamically generated within the chiral unitary approach (UChPT) from the final PP interaction, as explained in the Introduction. We will come back to the implementation of the FSI through the UChPT amplitudes in the second part of this section, but first, we address the calculation of the elementary production at the quark level in Fig. 1(a).

While the $\bar{d}$ quark remains as a spectator, the c quark becomes a d through the emission of a W boson, which eventually creates the $u\bar{s}$ of a K^+. Note that this process involves two Cabibbo suppressed weak transitions (Wcd and Wus). The final $\bar{d}d$ pair then hadronizes into a final pseudoscalar meson pair, which is implemented by

producing an extra $\bar{q}q$ with the $^3P_0$ model [62–64]. The weight of the different allowed pseudoscalar pairs produced in the hadronization can be related, up to a global normalization factor, using the following $SU(3)$ arguments.

Let $|H\rangle$ be the flavor state of the final hadronic part after the quark-antiquark pair is produced in the hadronization:

$$|H\rangle \equiv |d(\bar{u}u + \bar{d}d + \bar{s}s)\bar{d}\rangle. \tag{2}$$

It can be written as

$$|H\rangle = \sum_{i=1}^{3} |d\bar{q}_i q_i \bar{d}\rangle = \sum_{i=1}^{3} |M_{2i}M_{i2}\rangle = |(M^2)_{22}\rangle, \tag{3}$$

where we have defined

$$q \equiv \begin{pmatrix} u \\ d \\ s \end{pmatrix} \quad \text{and} \quad M \equiv q\bar{q}^{\mathsf{T}} = \begin{pmatrix} u\bar{u} & u\bar{d} & u\bar{s} \\ d\bar{u} & d\bar{d} & d\bar{s} \\ s\bar{u} & s\bar{d} & s\bar{s} \end{pmatrix}. \tag{4}$$

The strength of $SU(3)$ comes into play when we associate the matrix M to the usual $SU(3)$ matrix containing the pseudoscalar mesons,

$$M \Rightarrow P \equiv \begin{pmatrix} \frac{\pi^0}{\sqrt{2}} + \frac{\eta}{\sqrt{3}} + \frac{\eta'}{\sqrt{6}} & \pi^+ & K^+ \\ \pi^- & -\frac{1}{\sqrt{2}}\pi^0 + \frac{\eta}{\sqrt{3}} + \frac{\eta'}{\sqrt{6}} & K^0 \\ K^- & \bar{K}^0 & -\frac{\eta}{\sqrt{3}} + \frac{2\eta'}{\sqrt{6}} \end{pmatrix},$$

where we have used ideal mixing between the singlet and octet to give η and η' [65]. Then, the matrix element required in Eq. (3) is

$$(P^2)_{22} = \pi^-\pi^+ + \frac{1}{2}\pi^0\pi^0 + \frac{1}{3}\eta\eta - \sqrt{\frac{2}{3}}\pi^0\eta + K^0\bar{K}^0. \tag{5}$$

Note that, as mentioned above, no K^+K^- pair is possible in the hadronization from $\bar{d}d$, and then it must necessarily be produced in the final state interaction from the five possible pseudoscalar pairs, $\pi^-\pi^+$, $\pi^0\pi^0$, $\eta\eta$, $\pi^0\eta$, and $K^0\bar{K}^0$, as depicted in Fig. 2.

Note that we are not including the scalar $f_0(980)$ and $a_0(980)$ resonances as explicit degrees of freedom but they arise naturally in the nonlinear dynamics involved when implementing unitarity in coupled channels starting from a lowest-order tree-level meson-meson chiral potential. This effectively accounts for the resummation shown in Fig. 2, and it is the basis of the UChPT. In the scalar sector, there are several different ways to implement these ideas like the Bethe-Salpeter equation [49], the inverse amplitude method [24,66], or the N/D method [23], but all of them provide similar results. Since in the present work we are going to compare with experimental data from the LHCb
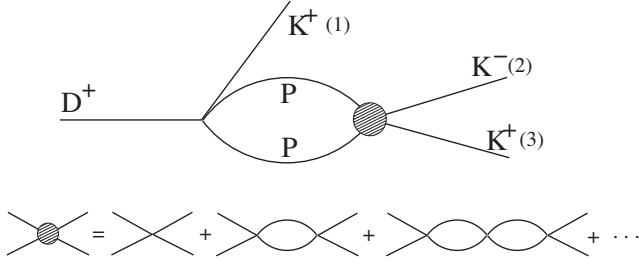
FIG. 2.   Final state interaction of the $D^+ \rightarrow K^+ PP$ process to get $D^+ \rightarrow K^- K^+ K^+$.

Collaboration, which involves $K^- K^+$ invariant masses up to 1375 MeV, we use the amplitudes from the N/D approach [23], which provides the largest range of predictability among the aforementioned approaches. All theses approaches rely upon mainly one free parameter coming from the regularization, either a cutoff or a subtraction constant, which is determined from a fit to meson-meson scattering data. The N/D method of Ref. [23] is able to extend the applicability range up to higher energies by including in the interaction kernel, in addition to the lowest-order ChPT amplitudes, the s-channel exchange of scalar resonances in a chiral symmetric invariant way. These tree-level resonances constitute an octet with mass around 1.4 GeV and a singlet around 1 GeV, which barely changes the dynamical origin of the $a_0(980)$ and $f_0(980)$ but improves the amplitude close to 1400 MeV. In any case, all of the UChPT approaches provide similar results in the region around 1 GeV. In Fig. 3, we show some spin 0 and isospin $I = 0$ and $I = 1$ meson-meson scattering amplitudes,[1] which will be needed in the present work. The energy range involved in the present work is from the $K^+ K^-$ threshold, 987 MeV, till $M_D - m_K = 1375$ MeV. We can clearly see the shapes for the $f_0(980)$ and $a_0(980)$, but note that these shapes are far from being just Breit-Wigners, and this is one of the strong points of UChPT; it provides not only the pole structure of the resonances but the actual scattering amplitude. The $a_0(980)$ actually corresponds to a cusp at the $K\bar{K}$ threshold.

We can then write the amplitude corresponding to the process in Fig. 2. If we use the label 1 for the K^+ coming directly from the D^+, label 2 for the K^-, and 3 for the other K^+ (see Fig. 2), it can be written as

$$T(s_{23}) = \mathcal{C} \sum_{i=1}^{5} h_i G_i(s_{23}) t_{i,K^+K^-}(s_{23}), \tag{6}$$

where $s_{ij} = (p_i + p_j)^2$. In Eq. (6), the sum runs over the five PP allowed channels in Eq. (5), $\mathcal{C}$ is an arbitrary global normalization factor to be fitted later on to the experimental

[1]In Fig. 1 of Ref. [67], a comparison with several scattering data obtained using these amplitudes can be seen.
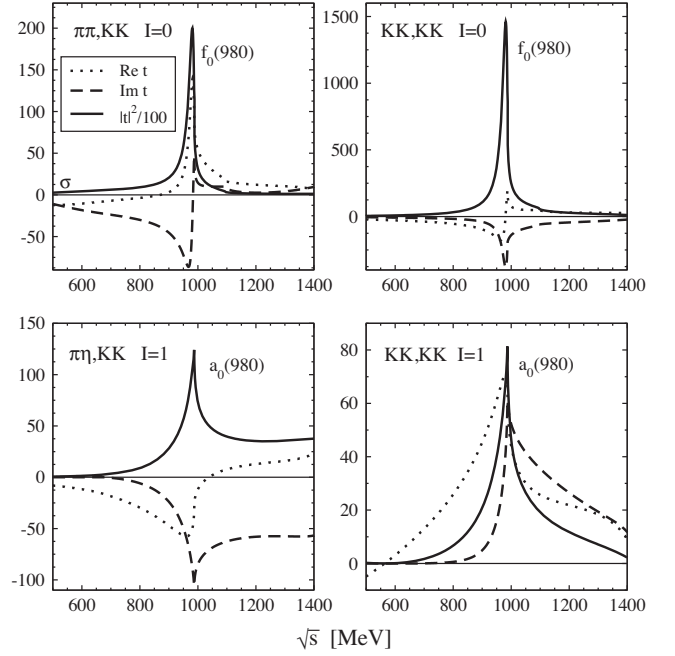

FIG. 3.   Meson-meson scattering amplitudes for isospin $I = 0$ and $I = 1$.

LHCb data, h_i are the numerical coefficients in front of each PP channel in Eq. (5), t_{i,K^+K^-} stands for the unitarized $(PP)_i \rightarrow K^+ K^-$ amplitude in the s wave explained above, and G_i is the loop function for two pseudoscalar mesons regularized with the same subtraction constant used in the evaluation of t_{i,K^+K^-}.

We can theoretically filter the different isospin contributions, taking into account that $\pi^- \pi^+$, $\pi^0 \pi^0$, and $\eta\eta$ contribute only to $I = 0$ and $\pi^0 \eta$ contributes only to $I = 1$. The $K^0 \bar{K}^0$ pair contributes to both isospins, but taking into account the isospin decomposition of the different $K\bar{K}$ states,

$$|K^+ K^-\rangle = -\frac{1}{\sqrt{2}} |K\bar{K}\rangle_{I=1,I_3=0} - \frac{1}{\sqrt{2}} |K\bar{K}\rangle_{I=0,I_3=0},$$

$$|K^0 \bar{K}^0\rangle = \frac{1}{\sqrt{2}} |K\bar{K}\rangle_{I=1,I_3=0} - \frac{1}{\sqrt{2}} |K\bar{K}\rangle_{I=0,I_3=0}, \tag{7}$$

it suffices to substitute, in Eq. (6),

$$t_{K^0 \bar{K}^0, K^+ K^-} \rightarrow \frac{1}{2} (t_{K^0 \bar{K}^0, K^+ K^-} + t_{K^+ K^-, K^+ K^-}) \tag{8}$$

for $I = 0$ and

$$t_{K^0 \bar{K}^0, K^+ K^-} \rightarrow \frac{1}{2} (t_{K^0 \bar{K}^0, K^+ K^-} - t_{K^+ K^-, K^+ K^-}) \tag{9}$$

for $I = 1$.

To the $I = 0$ amplitude in Eq. (6), we must add the contribution from the $\phi(1020)$ meson, which, being a

genuine $\bar{q}q$ resonance in the p-wave, is not included in the aforementioned meson-meson scattering amplitudes. Since the amplitude is going to span a large invariant mass region, we consider a full relativistic amplitude as in Ref. [12],

$$T_\phi(s_{23}, s_{12}) = \mathcal{D}\frac{s_{13} - s_{12}}{s_{23} - m_\phi^2 + im_\phi\Gamma_\phi(\sqrt{s_{23}})}, \quad (10)$$

where $s_{13} = M_D^2 + 3m_K^2 - s_{12} - s_{23}$, D is a complex arbitrary normalization factor to be fitted later on, and we use an energy-dependent p-wave ϕ width

$$\Gamma_\phi(m) = \Gamma_o \frac{m_\phi}{m}\frac{p^3(m)}{p^3(m_\phi)}B^2(m), \quad (11)$$

where Γ_o is the total width of the ϕ, $p(m)$ is the K momentum in the ϕ rest frame for a ϕ invariant mass m, and $B(m)$ is the p-wave Blatt-Weisskopf barrier penetration factor [68] given by

$$B(m) = \left(\frac{1 + (Rp(m_\phi))^2}{1 + (Rp(m))^2}\right)^{1/2}. \quad (12)$$

In Eq. (12), R stands for the range parameter of the ϕ a typical value of $R = 1.5$ GeV^{-1}, although it is not very relevant.

Finally, the three-body distribution for the $D^+ \to K^-K^+K^+$ decay is given by

$$\frac{d^2\Gamma}{ds_{12}ds_{23}} = \frac{1}{32(2\pi)^3 M_D^3}\frac{1}{2}|\mathcal{M}|^2, \quad (13)$$

where $\mathcal{M}$ is the total $D^+ \to K^-K^+K^+$ amplitude considered adding Eqs. (6) and (10), which must be properly symmetrized (exchanging the labels $1 \leftrightarrow 3$) since we have two identical K^+ in the final state,

$$\mathcal{M}(s_{23}, s_{12}) = T(s_{23}) + T_\phi(s_{23}, s_{12}) + (1 \leftrightarrow 3). \quad (14)$$

from where the K^+K^- spectrum can be obtained as

$$\frac{d\Gamma}{ds_{K^+K^-}} = \int_{s_{23}^{\min}}^{s_{23}^{\max}} ds_{23}\frac{d^2\Gamma}{ds_{12}ds_{23}}. \quad (15)$$

In the results section, we will also evaluate the K^+K^+ distribution, which is given by

$$\frac{d\Gamma}{ds_{K^+K^+}} = \int_{s_{23}^{\min}}^{s_{23}^{\max}} ds_{23}\frac{d^2\Gamma}{ds_{13}ds_{23}}, \quad (16)$$

This requires to write s_{12} in terms of s_{12} and s_{23}, which is done by means of $s_{12} = M_D^2 + 3m_K^2 - s_{13} - s_{23}$.

III. RESULTS

Our model has three parameters: one for the global normalization $\mathcal{C}$ in Eq. (6) and two for the global weight of the ϕ meson amplitude, complex $\mathcal{D}$ in Eq. (10), which we fit to the experimental [13] K^+K^- distribution [only Fig. 4(a)]. The other parts in Fig. 4 represent the K^+K^+ distribution and the distributions $s_{K^+K^-}^{\text{high}}$ and $s_{K^+K^-}^{\text{low}}$ where, according to Ref. [13], $s_{K^+K^-}^{\text{high}}$ and $s_{K^+K^-}^{\text{low}}$ represent the highest and lowest values among s_{12} and s_{23}; see Fig. 5. Theoretically, we evaluate the $s_{K^+K^-}^{\text{low}}$ distribution including $\theta(s_{23} - s_{12})$ in the integrand of Eq. (15), with θ the step function.

In all the figures, the dots represent the LHCb experimental data [13], the solid line represents our full model, the dotted line represents the phase-space, the dashed line represents the $I = 0$ contribution, and the dashed-dotted line represents the $I = 1$. The experimental data in Ref. [13] are not corrected for setup acceptance; however phase-space curves weighted by the efficiency for the different plots in Fig. 4 are provided in the experimental paper. Therefore, we have renormalized each experimental datum such that the phase space agrees with the theoretical three-body distribution.

A first observation from Fig. 4 is that our model fits reasonably well the whole spectrum of the K^+K^- and K^+K^+ distributions [recall that we have only fitted the data of Fig. 4(a)]. This is remarkable, given the little freedom in the fit: just the global normalization factor and the relative complex weight of the $\phi(1020)$. The rest is given from the nontrivial unitarization model implied in Eq. (6). It is also worth recalling again that there is no K^+K^- in the elementary production vertex of Fig. 1(a) and thus all the strength is coming from the FSI starting with meson-meson channels other than K^+K^-.

On the other hand, by looking at the different isospin contributions in Fig. 4, we see that the $I = 1$ contribution dominates over the $I = 0$ one. In particular, close to threshold, the accumulation of the strength with respect to the phase space is mainly due to the $I = 1$ amplitude, i.e., the effect of the $a_0(980)$. This is more clearly manifest if we look at Fig. 6, in which we zoom in the K^+K^- mass distribution near the threshold, including, in addition to the theoretical curves of Fig. 4(a), the contribution considering only the ϕ meson, only the $I = 0$ without the ϕ, and the full model removing the ϕ. This is also more clearly seen if we theoretically remove the phase space by plotting, in Fig. 7, the different isospin contributions from the FSI terms, i.e., without the ϕ, to the squared amplitude $|\mathcal{M}|^2$ of Eq. (13) without the $1 \leftrightarrow 3$ symmetrization, i.e., $\mathcal{M} \equiv T(s_{23})$, as a function of s_{23}. Note that if we included the ϕ meson or the symmetrization, the amplitude would also depend on the s_{12} variable. We see that close to threshold, indicated by the vertical dotted line, the strength is essentially dominated by the a_0 contribution. Below threshold, the shapes of the
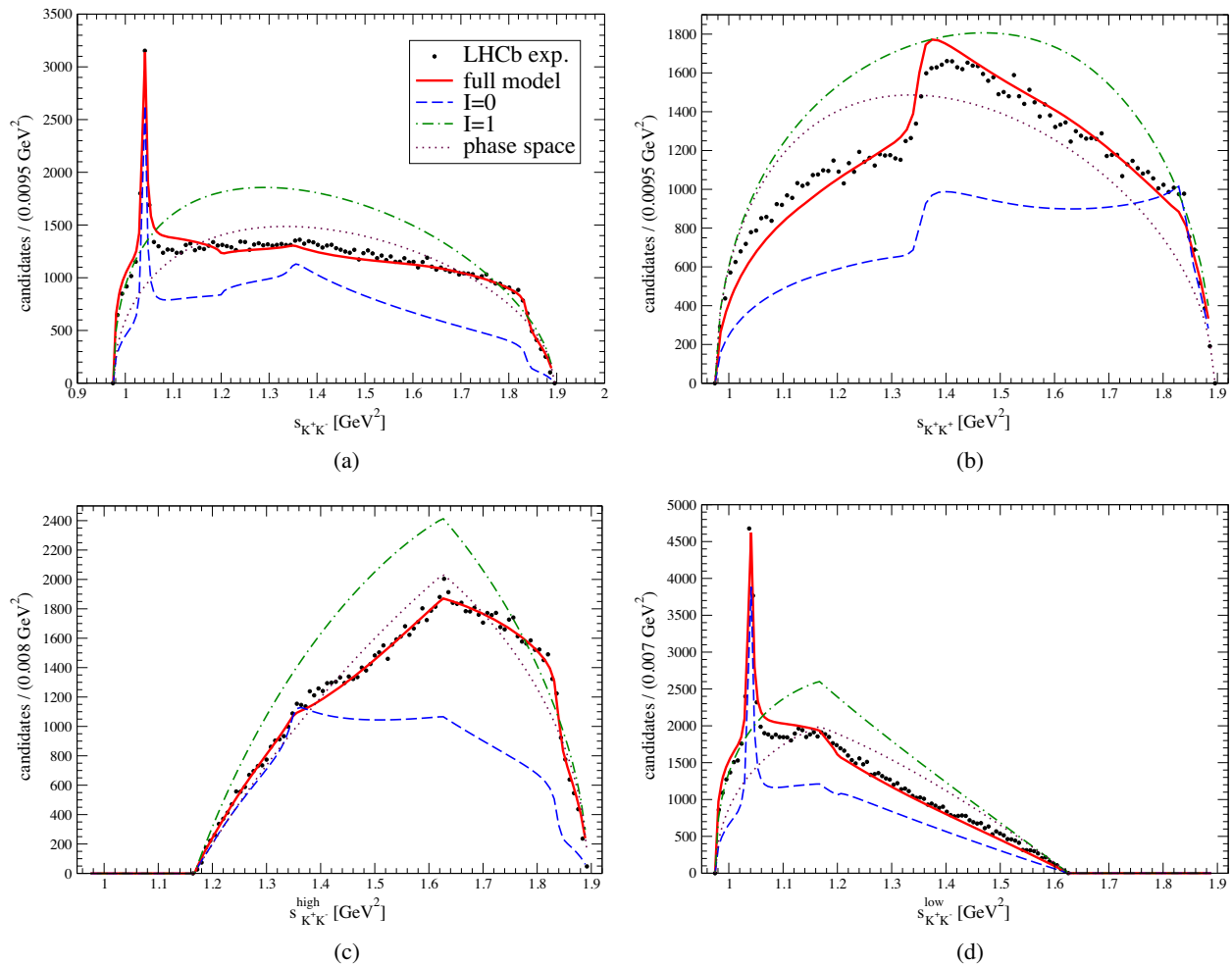
FIG. 4. Invariant mass distributions in comparison with the experimental data from Ref. [13].

a_0 and f_0 are clearly visible in this plot but are not accessible when considering the actual phase space. In Fig. 6, at low invariant masses, we see a pattern for the

$f_0(980)$ and $a_0(980)$ contributions different than what was found in Ref. [14]. In both approaches, a dominance of the $a_0(980)$ contribution is found. In Ref. [14], a destructive
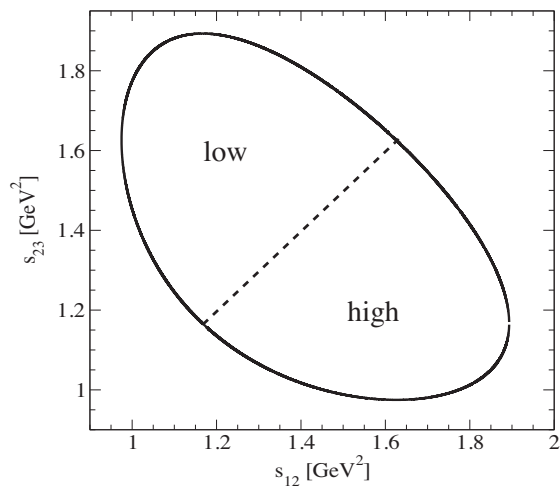
FIG. 5. Dalitz plot with the definition of the regions s_{12}^{high} and s_{12}^{low}.
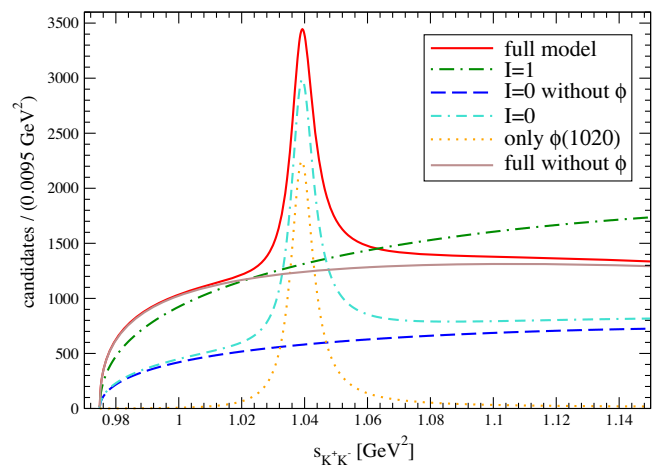
FIG. 6. Different contributions to the $D^+ \to K^- K^+ K^+$ mass distribution close to threshold.
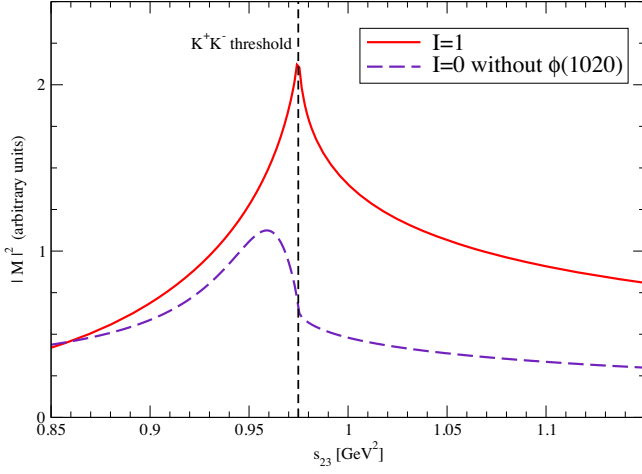
FIG. 7. Different isospin contributions to the $D^+ \to K^- K^+ K^+$ amplitude. The vertical dashed line represents the $K^+ K^-$ threshold.

interference between the a_0 and f_0 contributions was reported. We find a different pattern. The addition of the $f_0(980)$ resonance increases the contribution of the $a_0(980)$ at low invariant masses but subtracts for invariant masses higher than 1020 MeV. The interference of the $I = 0$ and $I = 1$ contributions is made possible in the present work because both contributions appear in the variables s_{12} and s_{23}.

IV. CONCLUSIONS

We show theoretically that the $D^+ \to K^- K^+ K^+$ decay can be understood from the mechanism that accounts for the final state interaction of an initial pseudoscalar pair [see Fig. 1(a)]. Indeed, $K^- K^+ K^+$ in the final state is not possible at the tree level, and hence the rescattering is mandatory. At this point, we take advantage of the unitary extensions

of chiral perturbation theory, which generate dynamically the $f_0(980)$ and $a_0(980)$ resonances, without the need to include them as explicit degrees of freedom, and provide the full meson-meson scattering amplitudes, not only the resonances. The relative weights of the initial production of the meson-meson pairs are obtained from SU(3) arguments, and then for the unitarization, we use the UChPT amplitudes from the N/D method, which allows us to extend the range of applicability to the whole final $K^+ K^-$ mass spectrum in this decay. With a minimal freedom, just the global normalization and the weight and phase of the $\phi(1020)$ contribution, we are able to fit experimental data on the $K^+ K^-$ invariant mass distribution. We also show that the dominant contribution close to threshold comes from the $I = 1$ [hence, the $a_0(980)$] contribution in clear dominance over the $I = 0$ one [the $f_0(980)$]. The remarkable agreement is a step in favor of considering this mechanism as the leading one in this decay, at odds with other considerations as in the experimental analysis [13] based on the work in Ref. [14], which advocates for the dominance of the mechanism in Fig. 1(b), and to reinforce the dynamical origin of the $a_0(980)$ and $f_0(980)$.

ACKNOWLEDGMENTS

[1] P. C. Magalhaes, M. R. Robilotta, K. S. F. F. Guimaraes, T. Frederico, W. de Paula, I. Bediaga, A. C. d. Reis, C. M. Maekawa, and G. R. S. Zarnauskas, Phys. Rev. D **84,** 094001 (2011).

[2] P. C. Magalhães and M. R. Robilotta, Phys. Rev. D **92,** 094005 (2015).

[3] D. R. Boito and R. Escribano, Phys. Rev. D **80,** 054007 (2009).

[4] M. Diakonou and F. Diakonos, Phys. Lett. B **216,** 436 (1989).

[5] J. P. Dedonder, R. Kaminski, L. Lesniak, and B. Loiseau, Phys. Rev. D **89,** 094018 (2014).

[6] J. J. Xie, L. R. Dai, and E. Oset, Phys. Lett. B **742,** 363 (2015).

[7] J. M. Dias, F. S. Navarra, M. Nielsen, and E. Oset, Phys. Rev. D **94,** 096002 (2016).

[8] R. Molina, J. J. Xie, W. H. Liang, L. S. Geng, and E. Oset, Phys. Lett. B **803,** 135279 (2020).

[9] Y. K. Hsiao, Y. Yu, and B. C. Ke, Eur. Phys. J. C **80,** 895 (2020).

[10] M. Y. Duan, J. Y. Wang, G. Y. Wang, E. Wang, and D. M. Li, Eur. Phys. J. C **80,** 1041 (2020).

[11] S. Sakai, E. Oset, and W. H. Liang, Phys. Rev. D **96,** 074025 (2017).

[12] G. Toledo, N. Ikeno, and E. Oset, arXiv:2008.11312.

[13] R. Aaij et al. (LHCb Collaboration), J. High Energy Phys. 04 (2019) 063.

[14] R. T. Aoude, P. C. Magalhães, A. C. Dos Reis, and M. R. Robilotta, Phys. Rev. D **98,** 056021 (2018).

[15] R. Aaij et al. (LHCb Collaboration), Phys. Rev. D **93,** 052018 (2016).

[16] D. Boito, J. P. Dedonder, B. El-Bennich, R. Escribano, R. Kaminski, L. Lesniak, and B. Loiseau, Phys. Rev. D **96,** 113003 (2017).

[17] K. S. F. F. Guimaraes, I. Bediaga, A. Delfino, T. Frederico, A. C. dos Reis, and L. Tomio, Nucl. Phys. B, Proc. Suppl. **199,** 341 (2010).

[18] F. Niecknig and B. Kubis, Phys. Lett. B **780,** 471 (2018).

[19] S. X. Nakamura, Phys. Rev. D **93,** 014005 (2016).

[20] A. M. Torres, K. P. Khemchandani, and E. Oset, Phys. Rev. C **77,** 042203 (2008).

[21] A. M. Torres, K. P. Khemchandani, L. Roca, and E. Oset, Few Body Syst. **61,** 35 (2020).

[22] G. Ecker, J. Gasser, A. Pich, and E. de Rafael, Nucl. Phys. **B321,** 311 (1989).

[23] J. A. Oller and E. Oset, Phys. Rev. D **60,** 074023 (1999).

[24] J. A. Oller, E. Oset, and J. R. Pelaez, Phys. Rev. D **59,** 074001 (1999); **60,** 099906(E) (1999); **75,** 099903(E) (2007).

[25] K. P. Khemchandani, A. M. Torres, H. Nagahiro, and A. Hosaka, Phys. Rev. D **88,** 114016 (2013).

[26] P. C. Magalhães, A. C. dos Reis, and M. R. Robilotta, Phys. Rev. D **102,** 076012 (2020).

[27] L. L. Chau, Phys. Rep. **95,** 1 (1983).

[28] R. J. Morrison and M. S. Witherell, Annu. Rev. Nucl. Part. Sci. **39,** 183 (1989).

[29] M. Ablikim et al. (BESIII Collaboration), Phys. Rev. Lett. **123,** 112001 (2019).

[30] E. Oset, W. H. Liang, M. Bayar, J. J. Xie, L. R. Dai, M. Albaladejo, M. Nielsen, T. Sekihara, F. Navarra, L. Roca et al., Int. J. Mod. Phys. E **25,** 1630001 (2016).

[31] E. van Beveren, T. A. Rijken, K. Metzger, C. Dullemond, G. Rupp, and J. E. Ribeiro, Z. Phys. C **30,** 615 (1986).

[32] E. van Beveren, D. V. Bugg, F. Kleefeld, and G. Rupp, Phys. Lett. B **641,** 265 (2006).

[33] F. E. Close and N. A. Tornqvist, J. Phys. G **28,** R249 (2002).

[34] J. R. Pelaez, Phys. Rev. Lett. **92,** 102001 (2004).

[35] D. Black, A. H. Fariborz, F. Sannino, and J. Schechter, Phys. Rev. D **59,** 074026 (1999).

[36] F. De Fazio and M. R. Pennington, Phys. Lett. B **521,** 15 (2001).

[37] R. A. Briceno, J. J. Dudek, R. G. Edwards, and D. J. Wilson, Phys. Rev. D **97,** 054513 (2018).

[38] N. N. Achasov and A. V. Kiselev, Phys. Rev. D **73,** 054029 (2006); **74,** 059902(E) (2006).

[39] N. N. Achasov and G. N. Shestakov, Phys. Rev. Lett. **99,** 072001 (2007).

[40] N. N. Achasov and A. V. Kiselev, Phys. Rev. D **83,** 054008 (2011).

[41] J. S. Schwinger, Ann. Phys. (N.Y.) **2,** 407 (1957).

[42] M. Gell-Mann and M. Levy, Nuovo Cimento **16,** 705 (1960).

[43] R. L. Jaffe, Phys. Rev. D **15,** 267 (1977).

[44] N. N. Achasov, S. A. Devyanin, and G. N. Shestakov, Phys. Lett. B **108,** 134 (1982); **108,** 435(E) (1982).

[45] N. N. Achasov and V. N. Ivanchenko, Nucl. Phys. **B315,** 465 (1989).

[46] N. N. Achasov and A. V. Kiselev, Phys. Rev. D **98,** 096009 (2018).

[47] N. N. Achasov, A. V. Kiselev, and G. N. Shestakov, Phys. Rev. D **102,** 016022 (2020).

[48] N. N. Achasov, J. V. Bennett, A. V. Kiselev, E. A. Kozyrev, and G. N. Shestakov, Phys. Rev. D **103,** 014010 (2021).

[49] J. A. Oller and E. Oset, Nucl. Phys. **A620,** 438 (1997); **A652,** 407(E) (1999).

[50] N. Kaiser, Eur. Phys. J. A **3,** 307 (1998).

[51] M. P. Locher, V. E. Markushin, and H. Q. Zheng, Eur. Phys. J. C **4,** 317 (1998).

[52] J. Nieves and E. Ruiz Arriola, Nucl. Phys. **A679,** 57 (2000).

[53] S. Weinberg, Phys. Rev. **166,** 1568 (1968).

[54] J. Gasser and H. Leutwyler, Ann. Phys. (N.Y.) **158,** 142 (1984).

[55] J. R. Peláez, A. Rodas, and J. R. de Elvira, arXiv: 2101.06506.

[56] J. A. Oller, E. Oset, and A. Ramos, Prog. Part. Nucl. Phys. **45,** 157 (2000).

[57] J. R. Pelaez, Phys. Rep. **658,** 1 (2016).

[58] F. K. Guo, C. Hanhart, U. G. Meißner, Q. Wang, Q. Zhao, and B. S. Zou, Rev. Mod. Phys. **90,** 015004 (2018).

[59] D. Gamermann, J. Nieves, E. Oset, and E. R. Arriola, Phys. Rev. D **81,** 014029 (2010).

[60] J. Yamagata-Sekihara, J. Nieves, and E. Oset, Phys. Rev. D **83,** 014003 (2011).

[61] M. Bayar, W. H. Liang, and E. Oset, Phys. Rev. D **90,** 114004 (2014).

[62] L. Micu, Nucl. Phys. **B10,** 521 (1969).

[63] A. Le Yaouanc, L. Oliver, O. Pene, and J. C. Raynal, Phys. Rev. D **8,** 2223 (1973).

[64] E. Santopinto and R. Bijker, Phys. Rev. C **82,** 062202 (2010).

[65] A. Bramon, A. Grau, and G. Pancheri, Phys. Lett. B **283,** 416 (1992).

[66] A. Dobado and J. R. Peláez, Phys. Rev. D **56,** 3057 (1997).

[67] J. A. Oller and L. Roca, Eur. Phys. J. A **34,** 371 (2007).

[68] J. M. Blatt and V. F. Weisskopf, Theoretical Nuclear Physics (Springer-Verlag, Berlin, 1979).